Int J Adv Manuf Technol
DOI 10.1007/s00170-012-3960-3

ORIGINAL ARTICLE

The harp: a vehicle crash test apparatus for full-scale crash test experiments

J. S. Johnsen · H. R. Karimi · K. G. Robbersmyr

Received: 2 October 2011 / Accepted: 29 January 2012

Abstract The current paper describes an apparatus for full-scale vehicle crash test experimentation. This apparatus is referred to as the harp. In brief, the harp may either accelerate a trolley which is impacted into a test vehicle or the test vehicle itself may be accelerated and impacted into an object such as a barrier, a pole, or another vehicle. If a trolley is accelerated, it is equipped with load cells to record the axial crushing force. If a test vehicle is accelerated, it is equipped with a three-axis accelerometer to record the crushing force. At the impact site, high-speed cameras and instrumentation record vital data during the crash.

Keywords Kicking machine · Impact testing · Structural components · The harp

Notation

m_p	total trolley mass
W	work done by an expanding gas
w_n	work done to pulley number (n)
p_1	initial pressure in the accumulator
p_2	final pressure in the accumulator
V_1	initial volume of gas in the accumulator
V	volume of gas in the accumulator
V_2	final volume of gas in the accumulator
γ	ratio of heat capacities
x_0	initial piston displacement
x	piston displacement
x_f	piston displacement at full stroke
A_p	accumulator piston area
K	total energy of the rotating arm
ω	angular velocity of the rotating arm
I	moment of inertia of the rotating arm
E	total energy of the trolley
v	velocity of the trolley

J. S. Johnsen · H. R. Karimi (✉) · K. G. Robbersmyr
Department of Engineering, Faculty of Engineering and Science, University of Agder,
4898 Grimstad, Norway
e-mail: hamid.r.karimi@uia.no

1 Introduction

During recent years, increased focus has been placed on vehicle crash safety. Today, a new car must undergo rigorous crash tests before it can be released into the market. These tests are undertaken by major companies operating large crash test facilities. Such facilities have not been readily available for universities and small companies that desire to engage in crash test research.

For the last two decades, an increasing number of research works have focused on developing theoretical crash test models. Lumped parameter modeling and finite element method (FEM) are two major approaches commonly used in vehicle crash modeling ([1–9]). A FEM model is capable of representing geometry and material details of a structure. The drawback of this method is the fact that it is costly (software and required hardware) and time consuming. Additionally, the cost and time of such simulation is increased by the extensive representation of the major mechanisms in the crash event. When using FEM models, it is desirable to compare their results with full-scale experimental measurements in order to enhance the simulation outcome—see [10]. Decomposition of a complicated mesh model of a car into less complex arrangements also produces satisfactory results—see [11]. Therefore, several theoretical crash test researches are conducted. The aim of these researches is to simulate a vehicle crash without having to perform one. However, it would be a desire to have a crash test apparatus capable of conducting full-scale crash

Published online: 26 February 2012

tests. Such an apparatus will enable testing in a controlled environment. The result of these experiments may be compared to results from mathematical crash test models. Such a comparison may reveal critical modeling parameters and verify the accuracy of the mathematical crash test models. On another active research frontier, there have been increasing research interests in dynamics analysis and collision warning systems for vehicles, see for instance [12–19].

The present paper describes how the harp can be used to accommodate the crash test research carried out at the University of Agder. Contrary to comparable crash test apparatuses, the harp does not require a large test facility. The harp may be placed in a small tower at the end of a parking lot and testing can be carried out in this parking lot. The harp can accommodate a variety of different experimental test setups. A crash trolley may be accelerated and crashed into a test specimen or the test vehicle itself may be accelerated and crashed into an object of interest such as a barrier, a pole, or another vehicle. If a crash trolley is used, crash test experiments may be carried out to the front, rear, and side of a test vehicle. If the test vehicle itself is accelerated, experiments may be carried out to the front and rear of the test vehicle. Under both circumstances, the crash may be head on or with a percentage of offset.

The great versatility of the harp renders it an important tool both for research and advanced product development. The following section describes the function of the harp. Further on, the efficiency of the harp is compared to a similar apparatus, the Kicking machine which is operated by SIMLab, Norwegian University of Science and Technology (NTNU).

2 The harp

The harp is basically a device which accelerates a crash cart or vehicle which then is crashed into an object of interest, e.g., a vehicle, pole, or barrier.

The accelerating system consists of a mast and an arm which rotates around a set of bearings in the plane of Fig. 1. The arm and the mast are connected by a hydraulic actuator which provides the force required to rotate the arm away from the mast. A cable is attached to the tip of the rotating arm and spanned between alternating pulleys on the mast and the arm. The other end of the cable is stretched across the test runway and attached to either a trolley or a test vehicle. When the hydraulic actuator rotates the arm away from the mast, the cable is reeled in and the trolley/vehicle is accelerated towards the impact site. The hydraulic actuator receives hydraulic fluid simultaneously from a hydraulic piston accumulator and a hydraulic power supply.

A proportional controller controls a servo valve which governs the hydraulic flow to the actuator and thus the velocity profile of the trolley/vehicle. When a predetermined

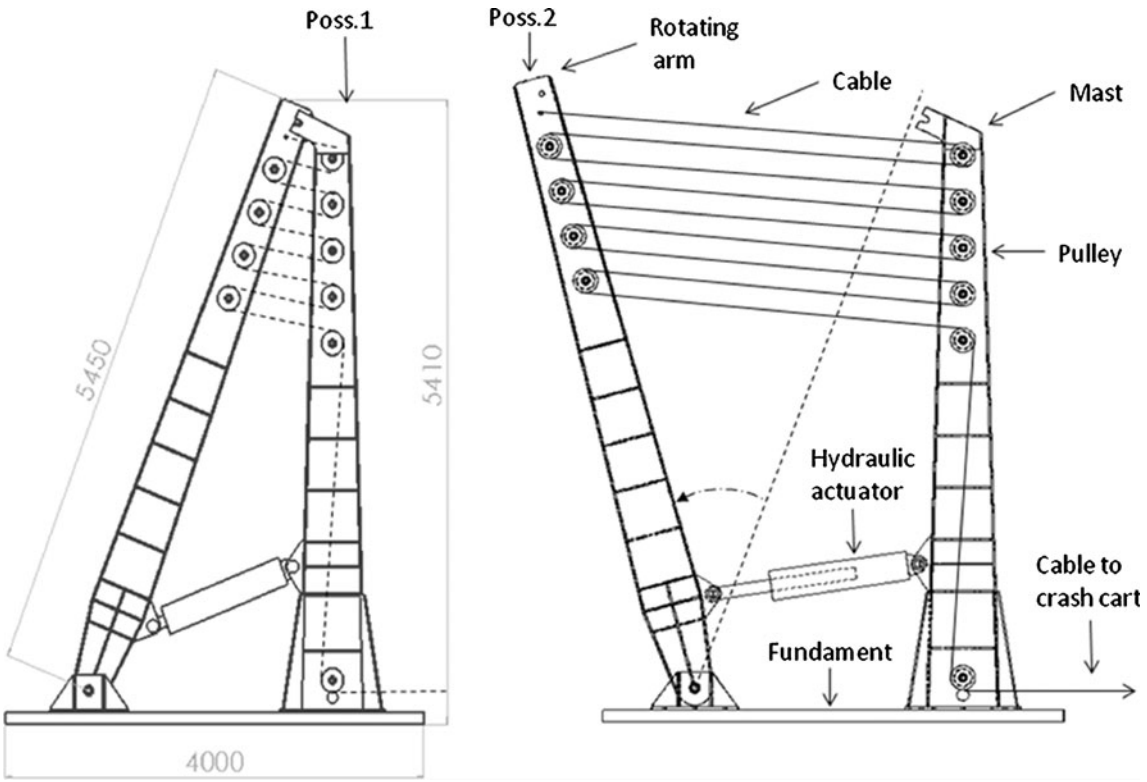

Fig. 1 An overview of the harp

velocity is reached, a release mechanism releases the cable. The trolley/vehicle coasts along its runway and impacts the object placed at the impact site. Sensors and instrumentation record vital crash data during the impact.

2.1 Principle of operation

Assume that the arm is in its starting position (Pos.1, Fig. 1). The arm is connected to the piston rod of a hydraulic actuator. Hydraulic fluid is delivered to the actuator simultaneously from a hydraulic piston accumulator and a hydraulic power supply. The rate of flow to the actuator is governed by a servo valve which is controlled by a proportional controller.

To prepare for a test a valve is opened to let fluid from the hydraulic power supply into the accumulator. The piston of the accumulator slowly rises from its bottom stop. The piston has reached its top stop when sudden rice in hydraulic pressure is indicated. The gas volume of the accumulator is now reduced from approximately 300 to 242 l. This compressed nitrogen is the energy source of the accumulator.

A test is started by opening the servo valve. Hydraulic fluid is delivered simultaneously from the hydraulic piston accumulator and the hydraulic power supply to the actuator. The actuator rotates the arm away from the mast (Pos.2, Fig. 1). A cable is spanned between the mast and the arm in a reversed tackle arrangement. This arrangement along with the leverage of the rotating arm introduces a 1:45 lever action. Thus, the force on the trolley/vehicle is 1/45 of the piston rod force, but the velocity of the trolley/vehicle is 45 times greater that the piston velocity. The cable is reeled in, and the trolley/vehicle which is attached to the end of the cable is accelerated towards the crash site.

The velocity profile of the trolley/vehicle is governed by a servo valve which is controlled by a proportional controller. The controller operates by comparing the angular velocity of the rotating arm to a preset angular velocity which results in a trolley/vehicle velocity 10% above the desired impact velocity. A cable release mechanism on the trolley/vehicle releases the cable at the desired impact velocity. This mechanism is incorporated to assure the correct impact energy. The trolley/vehicle coasts towards the crash site and impacts the test object.

2.2 Energy transformations

The main driving force of the kicking machine is compressed nitrogen in the accumulator. During the operation of the harp, energy is transformed from potential energy in the accumulator to impact energy at the crash site. The nitrogen of the accumulator has a maximum working pressure of 200 bars. During operation, the volume of the nitrogen expands from 242 to 300 l.

When calculating the energy output due to an expanding gas, it must first be determined what kind of thermodynamic process is occurring. In this case, the process may be considered to be adiabatic since the expansion occurs in such a short time interval. Secondly, it must be determined if the expanding gas may be considered as an ideal gas. In this case, the gas is nitrogen. Nitrogen is considered to obey an ideal gas model within a few present [20]. This justifies treating the nitrogen as an ideal gas in our further calculations. The work done by an ideal gas when expanding may be found by the following equation [20].

$$W = \frac{1}{\gamma - 1} \cdot (p_1 \cdot V_1 - p_2 \cdot V_2) \tag{1}$$

For nitrogen, the ratio of heat capacities is γ=1.40 at moderate pressure levels [20]. The final pressure in the accumulator p_2 must be found in order to calculate W. The following equation holds for an ideal gas during an adiabatic expansion.

$$p_1 \cdot V_1^{\gamma} = p_2 \cdot V_2^{\gamma} \tag{2}$$

Solving for p_2 yields

$$p_2 = p_1 \cdot \frac{V_1^{\gamma}}{V_2^{\gamma}} \tag{3}$$

Substituting Eq. 3 into Eq. 1 yields

$$W = \frac{1}{\gamma - 1} \cdot \left(p_1 \cdot V_1 - p_1 \cdot \frac{V_1^{\gamma}}{V_2^{\gamma}} \cdot V_2 \right) \tag{4}$$

Solving for W yields

$$W = 998\,kJ$$

Thus the maximum energy output of the accumulator is 998 kJ. In order to maximize the available impact energy, the actuator simultaneously receives energy from the accumulator and a hydraulic power supply. The power supply delivers 98 l/m at a pressure of 200 bar. If the cart/vehicle is to be accelerated up to 21 m/s in a distance of 40 m, this will take approximately 3.8 s. The hydraulic power supply can deliver approximately 124 kJ during this time. Thus, the total available energy is 1,122 kJ.

This energy is transformed towards the impact at the crash site. It is of importance that the energy is transformed as efficiently as possible. However, not all energy is transferred to the impact. The main contributors to energy "loss" during operation are:

1. internal friction in the cable
2. friction between the cable and the pulleys
3. increase in kinetic energy of the pulleys
4. friction in the pulley bearings

These losses will be related to the work done to each pulley during operation of the harp.

For each pulley, there is an incoming and an outgoing cable segment. When the cable travels around the pulley, there will be a slight increase in the tension in the cable. The work on each pulley is found by multiplying the difference in tension in the two cable segments by the length of the cable segment that travel around the respective pulley during operation. This is illustrated in Fig. 2.

In the industry, it has become customary to expect a 2% increase in cable tension when the cable travels 180° around a pulley of the size and setup which is used in the harp [22]. Since the cable only travels along 90° of the two lowest pulleys, these pulleys combined and treated as one pulley with a travel of 180°. This pulley is denoted pulley number 0. The rest of the pulleys are denoted from 1 to 8, where pulley number 8 is the uppermost pulley. Now, the total energy "loss" during operation may be found by adding the work done to each pulley.

$$w = \sum_{n=0}^{8} \Delta T_n \cdot l_n \tag{5}$$

Where, ΔT_n is the difference in tension in the incoming and outgoing cable of pulley number (n) and l_n is the length of the cable segment that travels around pulley number (n). The tension in each cable segment will depend on the force (F) which is exerted on the crash cart through the cable. The tension in the cable will increase by 2% for each pulley the cable travels around (pulley number 0 through 8). The length l_n will be halved each time the cable travels around a pulley situated on the rotating arm (pulley number 1, 3, 5, and 7). This is incorporated into Eq. 5 to get Eq. 6.

$$w = \sum_{n=0}^{8} (0.02 \cdot 1.02^n) \cdot F \cdot \left(\frac{1}{2}\right)^{\left\lfloor \frac{1}{2} \cdot n \right\rfloor} \cdot l \tag{6}$$

Remark 1 Equation (6) employs the FLOOR function with a nearest multiple of significance of 1 to the exponential term. This is done to assure that only the pulleys on the rotating arm halves the cables travel distance (l_n) around each pulley.

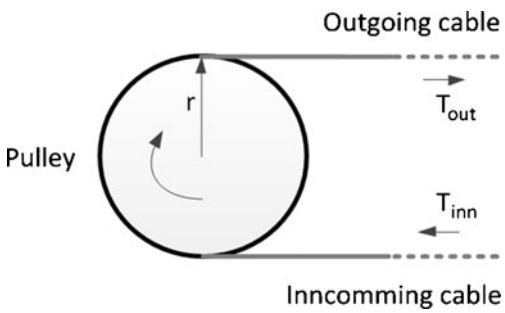

Fig. 2 Pulley and cable arrangement

Substituting $F = m_p \cdot a$ and $a = \frac{v^2}{2 \cdot l}$ into Eq. 6 yields.

$$w = \sum_{n=0}^{8} \frac{1}{2} m_p \cdot v^2 \cdot (0.02 \cdot 1.02^n) \cdot \left(\frac{1}{2}\right)^{\left\lfloor \frac{1}{2} n \right\rfloor} \tag{7}$$

$$w = \frac{m_p \cdot v^2}{100} \cdot \sum_{n=0}^{8} 1.02^n \cdot \left(\frac{1}{2}\right)^{\left\lfloor \frac{1}{2} \cdot n \right\rfloor} \tag{8}$$

Equation 8 will be the basis of calculating the energy "loss" during operation of the Harp as well as calculating the efficiency of the Harp. The next section presents the Kicking machine at SIMLab, NTNU. Further on the efficiencies of the Harp and the Kicking machine will be compared.

3 The kicking machine

Basically, the kicking machine accelerates a trolley on rails towards a test specimen fixed to a reaction wall. Figure 3 provides an overview of the kicking machine at SIMLab, NTNU.

The accelerating system consists of an arm that rotates around a set of bearings, i.e., the arm is free to rotate in the plane of Fig. 3. Note that the arm is open like a crankshaft at the bearing end. The arm itself is connected to a hydraulic/pneumatic actuator system, which provides the moving force. This system accelerates the trolley up to the desired impact velocity. The trolley traverses the length of the rails and subsequently hits the test specimen located at the far end [21].

3.1 Principle of operation

The arm is in its neutral position (Pos.1, Fig. 3). The arm is connected to the piston rod of a hydraulic/pneumatic actuator that is directly connected to a hydraulic accumulator of the piston type. The volume between the actuator piston and the accumulator piston is filled with hydraulic oil. A valve is opened to let pressurized air from the house mains into the piston rod side of the actuator. The arm moves slowly back as the excess oil from the actuator flows back to the tank of the hydraulic power supply. When the arm reaches its starting position (Pos. 2, Fig. 3), two hydraulic cylinders, one on each side, lock it by pressing against the locking plate. A valve is opened so that the volume on the rod side of the actuator is vented to the air. The trolley is now brought up snug against the arm. A thrust roller mounted at the rear of the trolley is in direct contact with the arm to ensure a perfect transfer of forces. The machine is then charged by pumping in hydraulic oil until the accumulator piston reaches its top position (against the top stops). This is indicated by a sudden rise in the oil pressure. The gas volume in the accumulator has now been reduced from approximately 200 to 161 l with a corresponding increase in pressure. This compressed gas is the energy source for the accelerating system. Hence, it is the initial gas pressure in the accumulator that

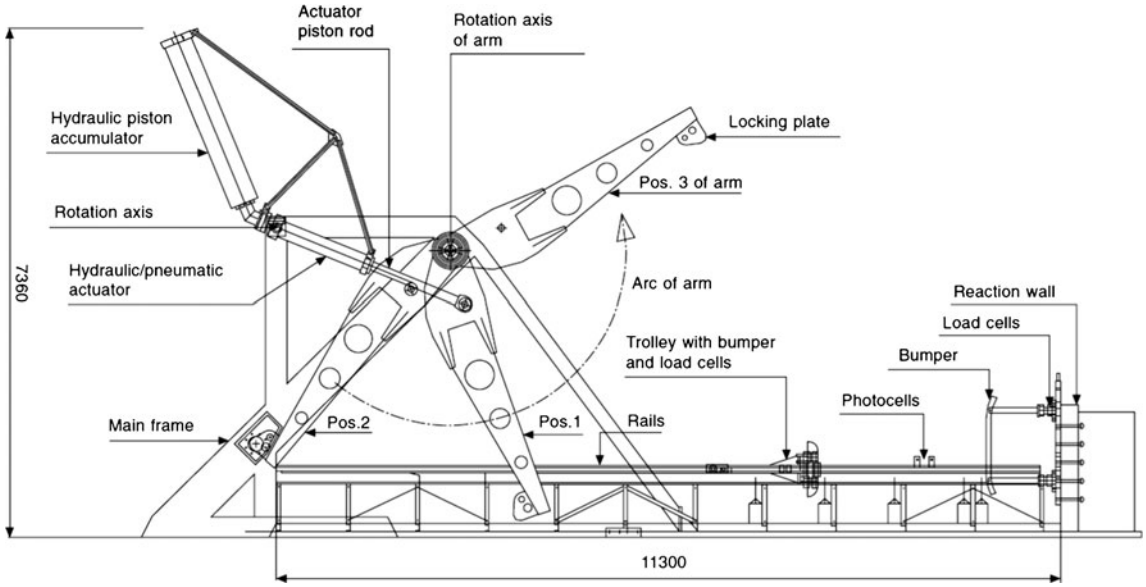

Fig. 3 The kicking machine at SIMLab, NTNU [21]

determines the force that can be produced. A test is started by releasing the hydraulic cylinders that locks the arm. The arm now pushes the trolley forward. The connection of the actuator piston rod to the arm introduces a 1:5 lever action, i.e., the force acting on the trolley is 1/5 of the piston rod force, but the velocity at the trolley level is five times greater. Once the arm has past the useful part of its arc, a sensor applies disk brakes in the arm hubs to stop the arm. After the test, the brakes are released and the arm dropped to its neutral position [21].

3.2 Energy transformations

The driving force of the kicking machine is compressed nitrogen in the accumulator. When the machine is fired, the compressed nitrogen has a maximum pressure of 200 bar. During the test, the volume of the nitrogen expands from 161 to 200 l. The energy output of the accumulator may be calculated by Eq. 4. This yields a maximum energy output of the accumulator of 670 kJ.

This energy is transformed towards the impact at the crash site. However, not all energy is transferred to the impact. The main contributors to energy "loss" during operation are:

1. energy remaining with the rotating arm after arm/trolley separation
2. energy delivered to the rotating arm after arm/trolley separation
3. friction in the thrust roller and bearings
4. air resistance of the rotating arm

When the kicking machine is fired, the energy in the accumulator is transferred to the actuator and further on to the rotating arm and trolley. The trolley is only receiving energy until the point where the trolley and rotating arm separates. Based on the schematics of the kicking machine [21], we conclude that separation occurs at 4/5 of the actuator piston stroke. Thus, we are interested in knowing what amount of energy has been delivered from the actuator at 4/5 stroke. To examine this, let us study the energy transfer from the accumulator to the actuator by assuming that:

1. The volume between the accumulator piston and the actuator piston is filled with an incompressible fluid (hydraulic oil).
2. There is no net mass flow to or from the volume between the two pistons.
3. All the energy delivered by the accumulator will be transferred to the actuator.

Based on these assumptions, we draw the conclusion that the displacement of the actuator piston must be proportional to the displacement of the accumulator piston. Thus, if we desire to calculate the energy delivered by the actuator at 4/5 of its stroke, we can do this by calculating the energy output of the accumulator at 4/5 of its stroke. First we must express the volumes V_1 and V_2 in Eq. 4 as a function of the accumulator piston displacements x_0 and x.

$$V_1 = A_p \cdot x_0 \tag{9}$$

$$V_2 = A_p \cdot x \tag{10}$$

Substituting Eqs. 9 and 10 into Eq. 4 yields

$$W = \frac{p_1 \cdot A_p}{\gamma - 1} \cdot \left(x_0 - x_0^{\gamma} \cdot \mathrm{x}^{1-\gamma}\right) \tag{11}$$

Let us assume A_p=0.0962 m^2, then x_0=1.674 m and x_f= 2.079 m. Also x=1.998 m at 4/5 stroke. Substituting into Eq. 11 yields.

$$W = 550\text{kJ}$$

Thus the energy delivered by the actuator at the time of trolley/arm separation is 550 kJ.

Remark 2 There does not exist a linear relationship between piston displacement x and accumulator energy output in Eq. 11. Thus, we could not have calculated the energy output at 4/5 stroke by simply multiplying the energy output at full stroke by 4/5.

The energy delivered from the actuator is transferred to the rotating arm and the trolley. Only the energy received by the trolley is transferred further to the impact. To examine this, let us study the moment where the trolley leaves the rotating arm by assuming that:

1. The trolley tangents the tip of the rotating arm imminent to the time of separation.
2. The potential energy of the rotating arm is the same at separation as at the start of the run, a minor inaccuracy.

Thus, the total energy of the rotating arm at the time of trolley/arm separation may be calculated by the following equation.

$$K = \frac{1}{2} \cdot I \cdot \omega^2 \tag{12}$$

The moment of inertia I of the rotating arm is not presented in the article so for the proceeding calculations it is assumed to be 3,097.7 kg m^2. This is based on a 3-D model of the arm (see Appendix). Based on the schematics of the Kicking machine [21], the angular velocity of the arm may be related to the velocity of the trolley at the time of separation by the following equation.

$$v = (4.10 \cdot \omega) \cdot \cos(52^\circ) \tag{13}$$

Substituting Eq. 13 into Eq. 12 yields an expression for the energy of the rotating arm at trolley/arm separation as a function of the trolley velocity.

$$K = \frac{1}{2} \cdot 0.157 \cdot I \cdot v^2 \tag{14}$$

The energy of the trolley at the time of separation may be calculated by the following equation.

$$E = \frac{1}{2} \cdot m \cdot v^2 \tag{15}$$

For the proceeding calculations, the mass of the trolley is assumed to be 794 kg as stated in [21].

4 Results

Equations 8, 11, 14, and 15 may be combined to obtain a graph which shows the required accumulator energy versus the desired impact energy for both the harp and the kicking machine. The result is shown in Fig. 4.

From Fig. 4, we can see that if an impact energy of 400 kJ is desirable, the kicking machine would require an accumulator capacity of approximately 625 kJ while the harp would only require a capacity of approximately 430 kJ. The kicking machine generally requires an accumulator capacity approximately 45% higher than that of the harp. Such a difference is of significance since an inefficient energy transformation will require an unrealistically large accumulator in order to achieve the relatively large impact energy required at the crash site.

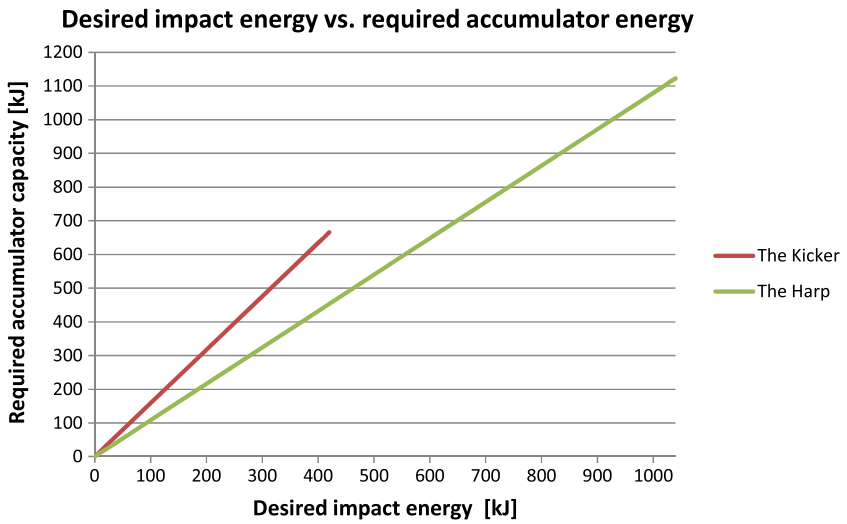

Fig. 4 Required accumulator energy vs. desired impact energy for a crash cart with a mass of 794 kg

Also it can be seen that the Harp is capable of delivering higher impact energy (1035 kJ) than the Kicking machine (425 kJ). The Harp can deliver almost 2.5 times the impact energy of the Kicking machine; there are three main reasons for this:

1. The Harp employs a 50% larger accumulator than the Kicking machine.
2. The Harp receives hydraulic fluid simultaneously from the accumulator and the hydraulic power supply during operation.
3. The Harp has a more efficient energy transformation than the Kicking machine.

Remark 3 The desired impact energy may be achieved by a variety of different crash cart masses and velocities; however, the results in Fig. 4 are only valid for a crash cart mass of 794 kg.

5 Discussion

The approach presented in this paper for calculating the impact energy of the kicking machine at SIMLab yields different results than those presented in the article on the kicking machine [21]. There seems to be three contributing factors to this.

1. In the article, the energy output of the accumulator is not calculated based on an adiabatic expansion of an ideal gas. This result in an overestimation of the energy output of the accumulator.
2. In the article, it is assumed that there exist a linear relationship between the stroke of the rotating arm and the energy output of the accumulator. Thus, the energy delivered at 2/3 stroke is calculated by multiplying the energy output at full stroke by 2/3.This results in an underestimation of the energy delivered by the actuator at trolley/arm separation.
3. In the article, it is assumed that all the energy delivered from the accumulator is transformed to the trolley. This results in an overestimation of the impact energy.

There are uncertainties associated with the moment of inertia of the rotating arm of the kicking machines. However, it would require a moment of inertia of less than 25% of what we estimated for us to get the same results as those presented in [21].

There are also uncertainties associated with the increase in tension that arise when the cable travel around the pulleys of the harp. However, even if the increase in tension was to be 100% higher than what we estimated, the energy "loss" during operation of the harp would only increase by approximately 4.4%. Therefore, it seems reasonable to assume that the efficiency of the energy transformation of the harp will be well above that of the kicking machine even if all uncertainties would appear to be in the harps disfavor.

Certain factors are not considered when calculating the energy transformations in both the harp and the kicking machine. These factors are described below.

1. Air resistance and friction on the crash cart. The Harp will most likely suffer the largest energy "loss" due to its longer runway.
2. Air resistance and bearing friction of the rotating arms. The Kicking machine will most likely suffer the largest energy "loss" due to the high velocity of its rotating arm and the friction between the arm and the thrust roller.
3. The changes in potential energy of the rotating arms. The Harp will most likely achieve a small increase in impact energy since the potential energy of the rotating arm decreases during operation.

From the schematics of The Harp and the Kicking machine (Figs. 1 and 3) it can be seen that the Harp is more compact and has a significantly smaller footprint than the kicking machine. This allows the harp to be located in a small tower at the end of the test runway. The omitted requirement for a large indoor test facility together with the harp's simplicity and ability to deliver high-impact energies in a variety of different crash test scenarios renders the harp ideal for small businesses and universities that desires to engage in vehicle crash test experimentation.

6 Conclusion

The major reason for the difference in results of this paper and those presented in the article [21] is due to the energy remaining in the rotating arm after trolley/arm separation. This is also the main reason for the higher efficiency in the energy transformation of the harp compared to the kicking machine. The energy which remains in the rotating arm is not contributing towards the energy at impact. This observation reveals two important issues when designing crash test apparatuses such as the harp and the kicking machine:

1. Any component receiving energy during the transformation of energy from the accumulator to the impact should be designed so as to transfer as large a quantity as possible of this energy further on towards the impact energy.
2. Any component receiving energy which cannot be passed further on to the impact energy should be designed so as to receive as small a quantity of energy as possible.

Table 1 Moment of inertia for different thicknesses of the rotating arm

Thickness (mm)	Mass (kg)	Moment of inertia (kg m^2)
20	555.28	1,548.84
30	832.92	2,323.27
40	1,110.56	3,097.7
50	1,388.17	3,872.12

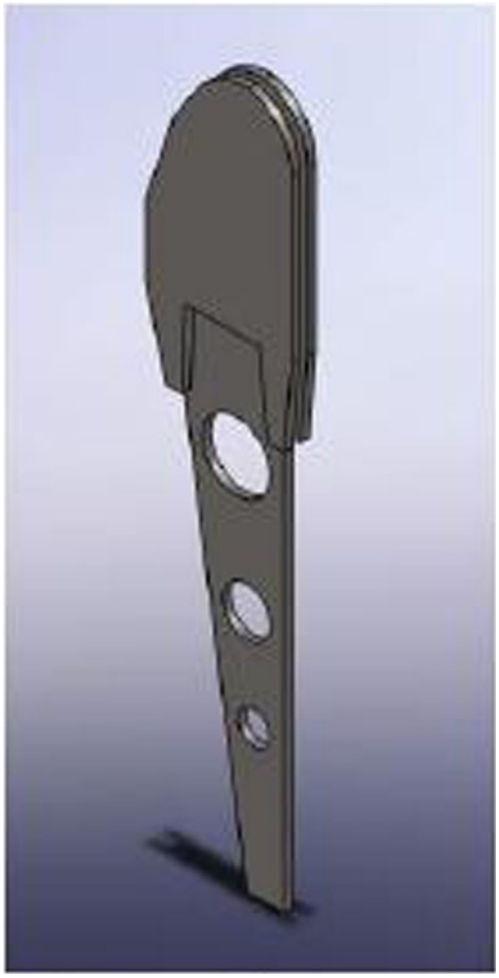

Fig. 5 3-D model of the rotating arm

Appendix A: 3-D model of the rotating arm

The rotating arm was modeled in solid works in order to estimate its moment of inertia. This was done because the moment of inertia was not reviled in the article on the kicking machine [21]. Although the general shape of the arm is known from the schematics of the kicking machine, there are uncertainties related to the thickness of the arm. For this reason the moment of inertia was calculated for various thicknesses. Finally, the moment of inertia corresponding to a thickness of 40 mm was selected. I=3097.7 kg m^2 (Table 1 and Fig. 5).

References

1. Belytschko T (1992) On computational methods for crashworthiness. Comput Struct 42(2):271–279
2. Jonsén P, Isaksson E, Sundin KG, Oldenburg M (2009) Identification of lumped parameter automotive crash models for bumper system development. Int J Crashworthines 14(6):533–541
3. Pawlus W, Nielsen JE, Karimi HR, Robbersmyr KG (2010) Mathematical modeling and analysis of a vehicle crash. The 4th European Computing Conference. Bucharest, Romania, April 20–22, 2010
4. Pawlus W, Nielsen JE, Karimi HR, Robbersmyr KG (2010) Development of mathematical models for analysis of a vehicle crash. WSEAS Trans Appl Theor Mech 5(2):156–165
5. Pawlus W, Nielsen JE, Karimi HR, Robbersmyr KG (2010) Further results on mathematical models of vehicle localized impact, The 3rd International Symposium on Systems and Control in Aeronautics and Astronautics, Harbin, China, June
6. Pawlus W, Karimi HR, Robbersmyr KG (2011) Application of viscoelastic hybrid models to vehicle crash simulation. Int J Crashworthiness 16(2):195–205
7. Pawlus W, Nielsen JE (2010) Development of mathematical models for vehicle to pole collision. Shaker Publishing, Maastricht. ISBN 978-90-423-0401-7
8. Pawlus W, Karimi HR, Robbersmyr KG (2011) Effects of different spring-mass model elasto-plastic unloading scenarios on the vehicle crash model fidelity. ICIC Express Letters, Part B: Applications 2(4):757–764
9. Pawlus W, Karimi HR, Robbersmyr KG (2010) Development of lumped-parameter mathematical models for a vehicle localized impact. Int J Adv Manuf Technol 3(2):57–77
10. Tenga TL, Changb FA, Liuc YS, Peng CP (2008) Analysis of dynamic response of vehicle occupant in frontal crash using multibody dynamics method. Math Comput Model 48(11–12):1724–1736
11. Moumni Z, Axisa F (2004) Simplified modelling of vehicle frontal crashworthiness using a modal approach. Int J Crashworthiness 9 (3):285–297
12. Li H, Liu H, Gao H, Shi P (2011) Reliable fuzzy control for active suspension systems with uncertainty of actuator delay and fault. IEEE Trans on Fuzzy Systems. doi:10.1109/TFUZZ.2011.2174244
13. Gao H, Sun W, Shi P (2010) Robust sampled-data H_∞ control for vehicle active suspension systems. IEEE Trans Cont Sys Tech 18 (1):238–245
14. Shen S, Wang J, Shi P, Premier C (2007) Nonlinear dynamics and stability analysis of vehicle plane motions. Veh Syst Dyn 45 (1):15–35
15. Hirose K, Toriu T, Hama H (2011) Estimation of vehicle wheelbase in a circular fisheye image using two-step detection method of tire-road contact points. Int J Innov Comput Inf Control 7 (8):4717–4728
16. Tseng SP, Liao Y-S, Lin C-W, Wang Y-L, Huang L-K (2010) A DSP-based lane recognition method for the lane departure warning system of smart vehicles. Int J Innov Comput Inf Control 6 (7):2985–2996
17. Chang Bao Rong, Young Chung-Ping, Tsai Hsiu Fen (2009) Simulation and implementation of high-performance collision warning system for motor vehicle safety using embedded ANFIS prediction. Int J Innov Comput Inf Control 5(10 (B)):3415–3430
18. Liu Fei, Liang Shan, Zhu Qin, Xiong Qinyu (2010) Effects of the consecutive speed humps on chaotic vibration of a nonlinear vehicle model. ICIC Express Letters 4(5(A)):1657–1664
19. Wu Y, Ji P, Wang T (2008) An empirical study of a pure genetic algorithm to solve the capacitated vehicle routing problem. ICIC Express Letters 2(1):41–45
20. Young HD, Freedman RA, Gaines JR, Palmer WF (1996) University physics, 9th edn. Addison-Wesley, New York
21. Hanssen AG, Auestad T, Tryland T, Langseth M (2003) The kicking machine: a device for impact testing of structural components. Int J Crashworthiness 8(4):385–392
22. API RP 9B (2011) Recommended practice on application care, and use of wire rope for oil field service, 13th edn. API Publishing Services